N_i = moles of component i formed by reaction
N_o = initial total moles
p_i = partial pressure of component i, mm. Hg
p_{io} = initial partial pressure of component i
P = total pressure, mm. Hg
P_o = initial total pressure
r = rate of reaction, g.-moles ethylamine/(g.-catalyst)(min.)
r_o, r_f = initial and final reaction rates

Subscripts

AN = acetonitrile
DEA = diethylamine
DEI = diethylimine
EA = monoethylamine
TEA = triethylamine

LITERATURE CITED

1. Restelli, E., Jr., and J. Coull, *AIChE J.*, **12**, 292 (1966).
2. Saunders, L. M., Ph.D. dissertation, Univ. Pittsburgh, Pa. (1963).
3. Kemball, C., and R. L. Moss, *Proc. Roy. Soc.* **A244**, 398 (1958).
4. Butt, J. B., Harding Bliss, and C. A. Walker, *AIChE J.*, **8**, 557 (1962).
5. Jones, A. M., Harding Bliss, and C. A. Walker, *ibid.*, **12**, 260 (1966).
6. Spry, J. K., personal communication.
7. Nogare, S. D., and R. S. Juvet, Jr., "Gas-Liquid Chromatography," p. 51, Interscience, New York (1962).
8. Pommersheim, J. M., Ph.D. dissertation, Univ. Pittsburgh, Pa. (1969).
9. Basila, M. R., personal communication.
10. Yang, K. H., and Hougen, O. A., *Chem. Eng. Progr.*, **46**, 146 (1950).
11. Peterson, E. E., "Chemical Reaction Analysis," p. 68, Prentice-Hall, Englewood Cliffs, N. J. (1965).
12. Reid, R. C., and T. K. Sherwood, "The Molecular Properties of Gases and Liquids," McGraw-Hill, New York (1958).
13. Benson, S. W., "Thermochemical Kinetics," Wiley, New York (1968).
14. Weisz, P. B., and C. D. Prater, "Advances in Catalysis," Vol. VI, p. 143, Academic Press, New York (1954).
15. Hougen, O. A., and K. M. Watson, "Chemical Process Principles," Vol. III, Wiley, New York (1947).
16. Brownlee, K. A., "Industrial Experimentation," Chemical Publishing, New York (1953).
17. Gregg, S. J., "The Surface Chemistry of Solids," p. 100, Reinhold, New York (1961).
18. Bond, G. C., "Catalysis by Metals," pp. 66-67, Academic Press, New York (1962).

Manuscript received August 28, 1969; revision received November 4, 1970; paper accepted November 5, 1970.

Dynamics of a Multiple-Effect Evaporator System

J. W. BURDETT and C. D. HOLLAND

Department of Chemical Engineering
Texas A&M University, College Station, Texas 77843

Presented is the development of a model for a system of evaporators at unsteady state operation, as well as a comparison of the dynamic behavior of the system predicted by the model with that observed in field tests. An objective of this project was to develop a suitable model of the process on the basis of the fundamentals of heat transfer, mass transfer, fluid flow, and the information commonly available from the design prints. The model predicts not only the dynamic behavior of the system to an upset in any of the operating variables but also the new steady state solution.

The field tests were made on the Freeport Demonstration Unit, located at Freeport, Texas. This plant was constructed under the direction of the Office of Saline Water, U. S. Department of the Interior. The details of the construction, operation, and successes achieved by this plant are well documented (*10, 12, 14, 26*).

The unit operation of evaporation is relatively old; yet many of the calculational procedures proposed by McCabe (*20*) in 1934 are still widely used. Principally, because of the need for fresh water, the evaporation process has enjoyed renewed interest in recent years (*1, 2, 9* to *12, 14* to *16, 18* to *21, 25* to *27*). Although numerous investigations on the dynamics of heat transfer and distillation processes have been reported (*7, 13, 17, 23, 24*), no study of the dynamics on a multiple-effect evaporator has been reported.

Correspondence concerning this article should be addressed to Professor C. D. Holland.

DESCRIPTION OF THE DESALINATION PLANT

A simplified flow diagram of the process appears in Figure 1. The design capacity of the plant was one million gallons per day, with a steam consumption of less than 0.08 lb. of supply steam per pound of gross product (*26*). The plant (see Figure 1) consisted of 17 effects of the long tube vertical (LTV) evaporator. The falling film version of the LTV evaporator was used. The first 12 effects of the plant were built as separate units, and each effect was sized according to its particular requirements. The last five effects were constructed in a single module.

Each evaporator consisted of a vertical shell-and-tube heat exchanger, which was mounted over a vapor-liquid separator. Noncondensables were removed continuously from each effect through the use of vapor bleeds, which were vented to the atmosphere, to the vapor space of the next effect, to the acid treater, or to the vacuum system. Most of the evaporators were equipped with 2-in. × 22 ft., 16 gauge tubes. The total areas for heat transfer varied from 3,000 to 4,000 sq. ft. per effect. Demister mats were used to prevent the entrainment of process liquid in the vapor leaving the sump of each evaporator. The process liquid entered the evaporator tubes through a suitably designed distirbutor at the top of each evaporator.

The feed (sea water) was heated slightly before it entered the acid treater (see Figure 1) where the carbon dioxide and dissolved air were removed. The seawater feed, acidified with sulfuric acid, entered the top of the tower through a full-cone nozzle, and was neutralized with caustic upon leaving the column. Steam from the steam bleed of effect 16 was introduced below the packing at a fixed flow rate. The vapor flow rate from the tower was controlled manually at a flow rate that was greater than the inlet vapor flow rate by an amount which would cause a temperature drop in the flashing feed of about 1°F.

In forward feed operation, the pretreated, preheated feed and steam from the supply line were charged to the first effect. Slightly concentrated process liquid was withdrawn from the sump of the first effect and charged as feed to the second effect. Vapors from the first effect became the steam for the second effect. The condensate leaving each effect was, of course, the desired product; however it contained sensible heat which was recovered in part by use of a heat exchanger at the first effect and by

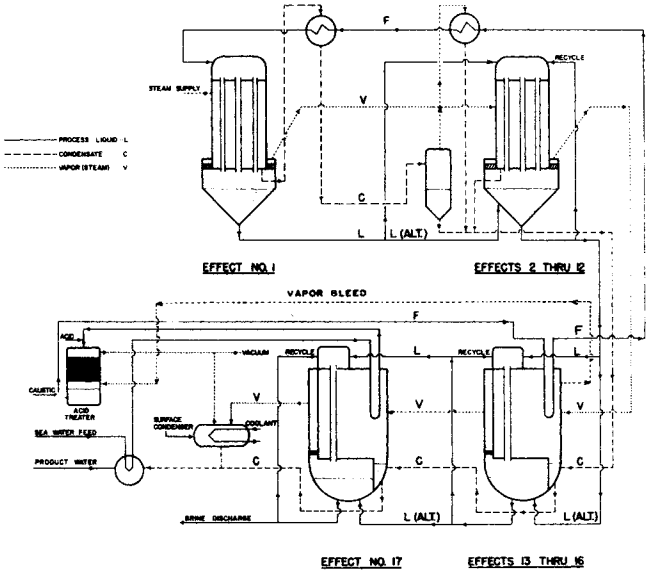

Fig. 1. Simplified flow diagram of the evaporator system.

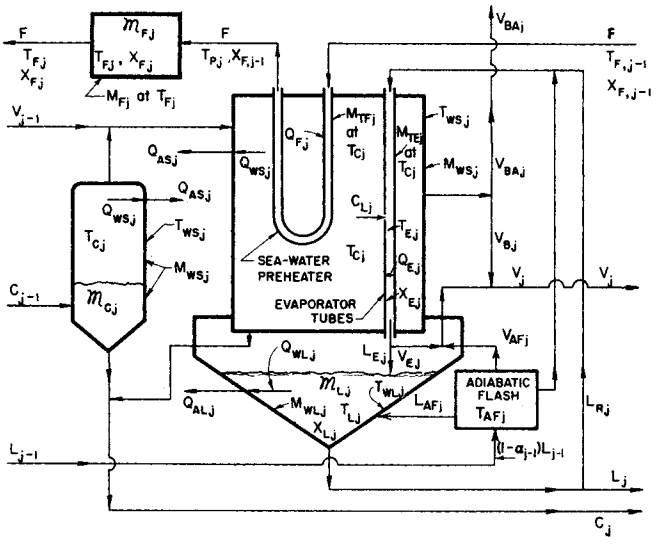

Fig. 2. Composite model for evaporator effect *j* and its associated auxiliary equipment.

flashing in the condensate-flash tanks at the subsequent effects.

Effects 10 through 17 had provisions for recycling liquid from the sumps of these effects to increase the liquid loading on the walls of the tubes. Effects 11 through 14 had alternate feed inlets which permitted sump-to-sump flow. Both of these options are shown in Figures 1 and 2 for effects 2 through 17, since these options were included in the mathematical model for all effects except the first.

Feed preheaters 1 through 12 were shell-and-tube heat exchangers. These preheaters were mounted vertically and adjacent to the evaporators; see Figures 1 and 2. Since the flow of steam to each preheater was unrestricted, the steam chest of each evaporator and the shell of its associated preheater were at the same pressure. Due to the piping configuration, condensate removal was self-regulating. Venting of the noncondensables was set by hand valves in the vent lines provided for each effect. Effects 2, 3, and 6 each had two preheaters with parallel steam flow and serial feed flow. In the model, each pair was treated as a single preheater. The feed preheaters for effects 13 through 17 were located within the steam chests of the respective effects, togeher with the evaporator tubes as indicated in Figures 1 and 2.

A detailed description of this plant, its equipment, and its operation (prior to the addition of the five-effect module) was given by Dykstra in 1965 (*10*). Additional details pertaining to both the 12- and 17-effect operations of the plant are available from the annual reports (*14*) by the operating company, Stearns-Roger Corporation, to the Office of Saline Water, U. S. Department of the Interior.

MODELING TECHNIQUES EMPLOYED

Since the heat transfer models utilized in the modeling of the desalination unit are applicable to numerous other processes, a brief development and analysis of these models follow.

Formulation of the Heat Transfer Model for Large Cylindrical Walls

By large cylindrical walls is meant that the thickness of the wall is small relative to the internal and external radii r_1 and r_2, respectively, so that the area term $2\pi rL$

in the rate expression

$$Q = -k2\pi rL\frac{dT}{dr} \tag{1}$$

may be approximated with good accuracy by use of either $2\pi r_1 L$ or $2\pi r_2 L$. It is further supposed that the length L is large so that a temperature gradient exists only in the direction of r.

The relatively large mass of metal contained in the system of evaporators represented an appreciable capacity for the storage of energy. This capacitance cannot be neglected in any realistic analysis of the dynamics of the process. However, the use of the classical equation for heat transfer by conduction at unsteady state [see Equation (5)] in the analysis would result in a tremendous task. To reduce the amount of effort required in the analysis, an approximate model for the transfer of heat through large cylindrical walls at unsteady state was employed.

The proposed model makes use of the fact that at steady state, the mean temperature T_m at which the heat content of the walls should be evaluated is approximately equal to the arithmetic average of the internal and external surface temperature T_1 and T_2. This equality $T_{av} = T_m$ is readily shown (3).

The model was formulated such that the condition $T_{av} = T_m$ is satisfied at steady state operation. In particular, let one half of the thermal resistance of the metal wall be concentrated at $r = r_1$ and the other half at $r = r_2$. These thermal resistances are called effective thermal conductivity films, and they are assigned zero masses. Then the thermal resistance per film is given by

$$\left.\begin{matrix}\text{Resistance per}\\ \text{effective thermal}\\ \text{conductivity film}\end{matrix}\right\} = \frac{1}{2}\left[\frac{r_2 - r_1}{k2\pi r_1 L}\right] \tag{2}$$

The film coefficient corresponding to this equivalent resistance is given by

$$h_e = \frac{2k}{(r_2 - r_1)} \tag{3}$$

The heat transfer model and its corresponding temperature profile at steady state are shown in Figure 3. Examination of this model shows that at steady state, it provides the correct wall temperatures needed in the formulation of the rates of heat transfer to and from the wall as well as the correct heat content of the metal wall.

For the case where no approximations are made with respect to the relative sizes of r_1 and r_2, appropriate expressions for T_m and the resistances of the effective thermal conductivity films have been developed by Burdett (3).

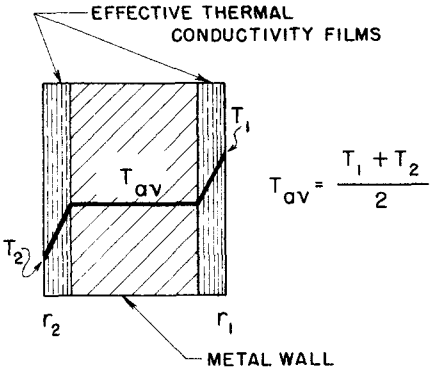

Fig. 3. Temperature profile predicted for large cylindrical walls ($r_2/r_1 \cong 1$ and the length along the cylindrical axis is large) at steady state.

$$\frac{1}{h_1} = \frac{l_{\text{ins.}}A}{(kA)_{\text{ins.}}} + \frac{A}{(hA)_{\text{air}}} \tag{4}$$

where A is the internal surface of the cylindrical section of metal wall, the subscript *ins.* refers to the insulation, and the subscript *air* refers to the air film.

At time $t = 0$ the metal wall is at the uniform temperature T_A of the surroundings, and at time $t = 0+$ the steam (with the saturation temperature T_S) is turned on. The corresponding partial differential equation is given by

$$\frac{\partial T}{\partial t} = \alpha\frac{\partial^2 T}{\partial x^2}, \quad (0 < x < l,\ t > 0) \tag{5}$$

where $\alpha = k/\rho C_V$. The boundary conditions are as follows:

$$k\frac{\partial T}{\partial x} - h_1(T - T_A) = 0, \quad (x = 0,\ t > 0)$$

$$k\frac{\partial T}{\partial x} + h_2(T - T_S) = 0, \quad (x = l,\ t > 0) \tag{6}$$

$$T = T_A, \quad (t = 0, \text{ for all } x)$$

The following solution to this problem is readily deduced from the result given by Carslaw and Jaeger (6) (case IX on page 126).

$$\frac{T(x,t) - T_A}{T_S - T_A} = a\left(x + \frac{1}{H_1}\right) - \sum_{n=1}^{\infty} C_n D_n Y_n(x) e^{-\alpha\beta_n^2 t} \tag{7}$$

where

$$C_n = \frac{[2(\beta_n^2 + H_2^2)]^{1/2}}{\beta_n\{(\beta_n^2 + H_1^2)[l(\beta_n^2 + H_2^2) + H_2] + H_1(\beta_n^2 + H_2^2)\}^{1/2}};$$

Comparison of the Temperatures Predicted by the Heat Transfer Model at Unsteady State with the Theoretical Values

In the following comparisons, it is supposed that the ratio r_2/r_1 is approximately equal to unity. Consider the boundary-value problem having the boundary conditions depicted in Figure 4. This problem corresponds to the case of a metal wall in contact with steam at $x = l$ and the surroundings at $x = 0$. At $x = l$, the steam film coefficient is denoted by h_2 and the steam temperature by T_S. At $x = 0$, an effective film resistance is used to represent the combined resistance offered by the insulation and the air film to heat transfer. The effective film resistance is denoted by $1/h_1$ and defined by

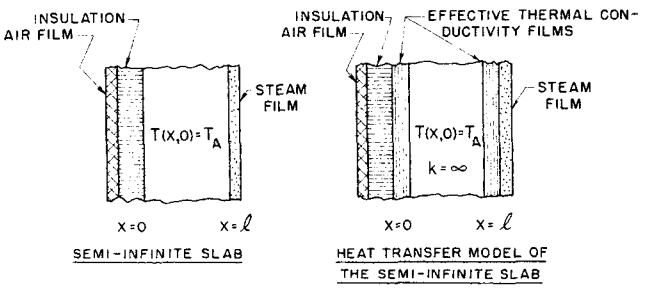

Fig. 4. Heat transfer model of a semi-infinite slab in contact with air on the insulated side and steam on the other side.

$$a = \frac{1}{\frac{1}{H_1} + \frac{1}{H_2} + l}, \quad H_1 = h_1/k, \quad H_2 = h_2/k;$$

$$D_n = [H_2 \cos \beta_n l]\left[\frac{\beta_n^2 + H_1^2}{\beta_n^2 - H_1 H_2}\right];$$

$$Y_n(x) = \beta_n C_n[\beta_n \cos \beta_n x + H_1 \sin \beta_n x];$$

$\beta_1, \beta_2, \ldots, \beta_n$ = first n positive roots of

$$(\beta^2 - H_1 H_2) \sin \beta l - \beta(H_1 + H_2)\cos \beta l = 0.$$

The result given by Equation (7) may be used to determine the mean temperature $T_m(t)$ which is required to give the correct heat content of a finite section of the slab at any time $t > 0$ as follows:

$$T_m(t) - T_A = \frac{1}{l}\int_0^l [T(x\,t) - T_A]dx \qquad (8)$$

When the integrand $[T(x, t) - T_A]$ is replaced by its equivalent as given by Equation (7) and the indicated integration is caried out, the result so obtained may be rearranged to give

$$\frac{T_m(t) - T_A}{T_S - T_A} = a\left(\frac{1}{H_1} + \frac{l}{2}\right) - \frac{1}{l}\sum_{n=1}^{\infty} C_n^2 D_n(D_n + H_1)e^{-\alpha\beta_n^2 t} \qquad (9)$$

For the boundary-value problem under consideration, the differential equation of the corresponding heat transfer model (see Figure 4) is given by

$$U_2(T_S - T) - U_1(T - T_A) = l\rho C_v \frac{dT}{dt} \qquad (10)$$

where

$$\frac{1}{U_1} = \frac{l_{\text{ins.}}A}{(kA)_{\text{ins.}}} + \frac{A}{(hA)_{\text{air}}} + \frac{l}{2k}; \quad \frac{1}{U_2} = \frac{1}{h_{\text{steam}}} + \frac{l}{2k}.$$

Separation of the variables in Equation (10), followed by integration and rearrangement, yields

$$\frac{T(t) - T_A}{T_S - T_A} = \left(\frac{U_2}{U_1 + U_2}\right)\left[1 - e^{-\left(\frac{U_1 + U_2}{l\rho C_V}\right)t}\right] \qquad (11)$$

A comparison of the values of $T_m(t)$ predicted by the heat transfer model as given by Equation (11) with the theoretical values given by Equation (9) is presented in Figure 5. The heat transfer coefficients and other parameters used to compute the results shown in this figure were of the same order of magnitude as those for the system of evaporators under consideration.

A Limiting Case for the Heat Transfer Model

The boundary-value problem corresponding to an evaporator shell with a perfect insulator on one side and steam with an infinite film coefficient on the other side is depicted in Figure 6. The postulate of an infinite value of the steam film coefficient amounts to taking the surface temperature of the wall on the steam side equal to the saturation temperature T_S of the steam. The partial differential equation is again given by Equation (5), and

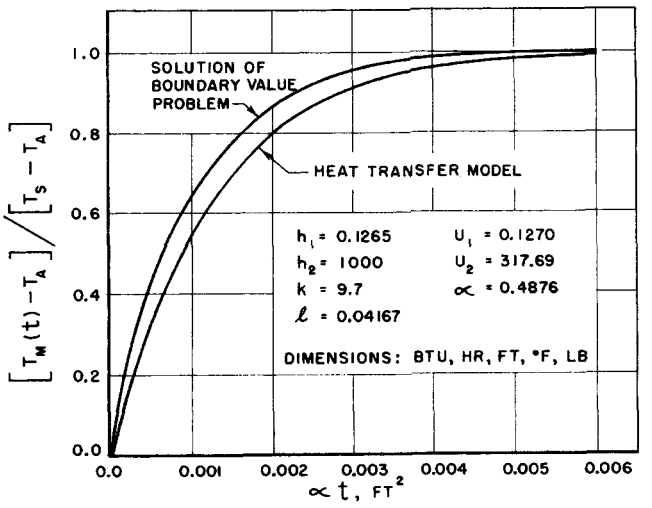

Fig. 5. Comparison of the results given by the heat transfer model with those given by the solution of the corresponding boundary-value problem (see Figure 4).

the boundary conditions are as follows:

$$T(x, 0) = T_A, \quad (0 < x < l)$$

$$\frac{\partial T(0, t)}{\partial x} = 0, \quad (t > 0)$$

$$T(l, t) = T_S, \quad (t > 0)$$

The solution satisfying both the partial differential equation and the boundary conditions may be stated in terms of either a Fourier series of cosines or a series of complementary error functions (6, 8). Of these two forms of the solution, only the later is given because it is said to converge (4) more rapidly for small values $\alpha t/l^2$.

$$\frac{T_S - T(x, t)}{T_S - T_A} = 1 - \sum_{n=0}^{\infty}(-1)^n \left\{\text{erfc}\frac{(2n+1)l - x}{2(\alpha t)^{1/2}} + \text{erfc}\frac{(2n+1)l + x}{2(\alpha t)^{1/2}}\right\} \qquad (12)$$

The result given by Equation (12) may be used to determine that mean temperature which is required to give the correct heat content of a section of the slab in a manner analogous to that demonstrated for Equation (8). The corresponding result is given by

$$\frac{T_m(t) - T_A}{T_S - T_A} = 2\left(\frac{\alpha t}{l^2}\right)^{1/2}\left\{\pi^{-1/2} + 2\sum_{n=1}^{\infty}(-1)^n \text{ierfc}\frac{nl}{(\alpha t)^{1/2}}\right\} \qquad (13)$$

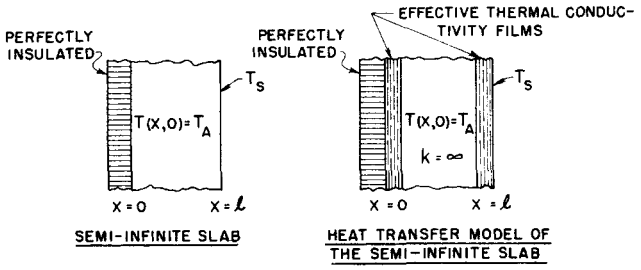

Fig. 6. Heat transfer model of a semi-infinite slab which is perfectly insulated at one end and the temperature is constant at the other.

Values of ierfc z have been tabulated by Carslaw and Jaeger (6).

For the boundary-value problem under consideration, the differential equation of the corresponding heat transfer model (see Figure 6) is given by

$$\frac{2k}{l}(T_S - T) = l\rho C_V \frac{dT}{dt} \tag{14}$$

Separation of the variables followed by integration and rearrangement yields

$$\frac{T(t) - T_A}{T_S - T_A} = 1 - e^{-\frac{2\alpha t}{l^2}} \tag{15}$$

A comparison of the theoretical values of the temperature ratio given by Equation (13) with those predicted by use of Equation (15) appears in Figure 7.

Errors in the Mean Temperatures Predicted by the Heat Transfer Model for Large Cylindrical Walls

The solutions given by Equations (9) and (11) correspond to a system having conditions which are far more severe than any which existed during the test runs. The boundary conditions [see Equation (6)] suppose that the initial temperature of the metal at the time of the upset is equal to the temperature T_A of the surroundings. To obtain some idea of the difference in the mean temperatures of the wall given by the solution of the boundary-value problem [see Equation (9)] and the heat transfer model [Equation (11)]; consider the case where $T_A = 80°F.$ and $T_S = 250°F.$ That is, the initial temperature of the metal and the surroundings is 80°F. and time $t = 0$, one side of the metal wall is suddenly exposed to saturated steam at 250°F. The initial time step used in the program for the system was 0.5 min. Then for $t = 1/120$ hr., the following results are obtained from Figure 5: the solution of the boundary-value problem gives $T_m = 248°F.$ and the solution of the heat transfer model gives $T_m = 243°F.$

The boundary conditions given above Equation (12) are also more severe than those which existed during the test run. For purposes of illustration, consider the case where the initial temperature T_A of the metal is 240°F. and the temperature T_S of the steam in contact with one side of the wall is suddenly changed to 270°F. [In the actual upset (see Figure 12*), the steam temperature changed only 0.5°F. during the first time step of 0.5 min. after the upset in the flow rate of the steam.] At the end of 1/120 hr., the mean temperature given by the solution of the boundary-value problem is $T_m = 269.90°F.$, and the solution for the heat transfer model is $T_m = 269.72°F.$ These results may be obtained by use of the Equations (13) and (15).

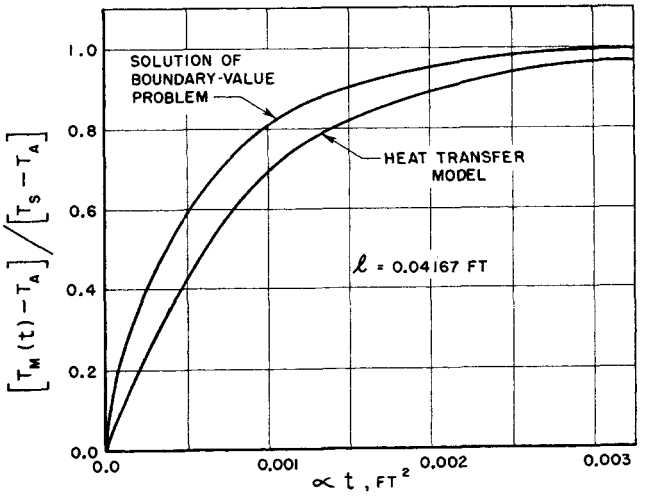

Fig. 7. Comparison of the results given by the heat transfer model with those given by the solution of the corresponding boundary-value problem (see Figure 6).

Heat Transfer Model for the Tubing of the Steam-heated Heat Exchangers

The proposed model for the thin metal walls consists simply of taking the mean temperature of the walls equal to the steam temperature. For the case of thin walls such as those found in the steam-heated heat exchangers, the mean temperature found by solving the boundary-value problem is approximately equal to the wall temperature predicted by use of the heat transfer model.

Heat Transfer Model for the Liquid in the Feed Preheaters

The proposed model for the liquid in the feed preheaters consists of the use of the steady state relationships to describe the rate of heat transfer occurring at the beginning and at the end of any time period during the transient analysis of the process model. Support for this model is the fact that the process fluid undergoes plug flow through the tubes with little axial mixing, and the fact that the residence time of the fluid in the exchanger was short compared with the time intervals used in the numerical solution for the system of evaporators.

FORMULATION OF THE MODEL FOR THE SYSTEM OF EVAPORATORS

First a statement of the assumptions upon which the model is based is presented, and then equations typical of those required to describe the model are presented.

1. The masses of metal in evaporator tubes and in the feed preheater tubes are denoted by M_{TEj} and M_{TFj}, respectively. These masses of metal are taken to be at the temperature T_{Cj} of the condensing steam in effect j. This approximation is based on the fact that the steam film coefficient was relatively large compared with the liquid film coefficient, and the fact that the tube walls were relatively thin. The tubes and the heat transfer model are displayed in Figures 1, 2, and 18.*

2. The mass of metal M_{WSj} of each evaporator effect j which is exposed to condensing steam or condensate on one side and the suroundings on the other is assigned the temperature T_{WSj} (see Figure 19*). One-half of the thermal resistance of the metal wall is assigned to an equivalent film on each side of the wall.

3. The holdup of energy by the insulation was taken to be negligible relative to the holdup of energy by the feed, process liquid, condensate, and metal in the evaporator system. This approximation rests primarily on the fact that the actual mass of the insulation was relatively small.

4. The mass of metal M_{WLj} of each effect j which is in contact with the process liquid on one side and the surroundings on the other is taken to be at the temperature T_{WLj} (see Figure 20*).

5. The discharge temperature T_{Ej} of the process liquid

* A statement of the complete set of equations, a description of Test Run No. 2, Figures 11 through 25, Tables 3 through 19, and a generalized scaling procedure for the Raphson method has been deposited as documents 01455 and 01457 with the ASIS National Auxiliary Publications Service, c/o CCM Information Sciences, Inc., 909 Third Ave., New York 10022 and may be obtained for $2.00 for microfiche or $5.00 for photocopies.

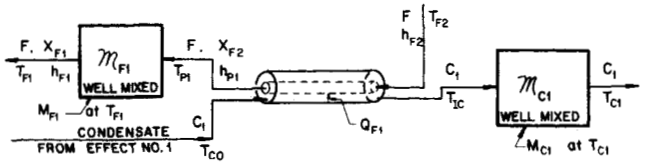

Fig. 8. Models for the condensate holdup and feed preheater for the first effect.

from the tubes is computed by use of Dühring lines based on the condensate temperature of the next effect and the mass fraction X_{Ej} of salt in the liquid discharged from the tubes of evaporator effect j; see Figure 21.*

6. The pressure drop between the sump of one effect and the steam chest of the next effect is taken to be negligible.

7. In the rate expression for the transfer of heat from the condensing steam at temperature T_{Cj} to the process liquid flowing down through each evaporator tube, the discharge temperature T_{Ej} of the process liquid is used in the potential term $(T_{Cj} - T_{Ej})$. This approximation is consistent with the fact that the heat transfer coefficient U_{Ej} employed was calculated at steady state operation on the basis of the discharge temperature.

8. The accumulation of mass or energy of process liquid in the evaporator tubes is taken to be negligible relative to the accumulation of mass or energy of process liquid in the sump of effect j.

9. The total amount of steam condensate associated with each effect is denoted by $\mathcal{M}_{Cj}$; see Figures 2 and 8. Except for the first effect the mass of condensate $\mathcal{M}_{Cj}$ is taken to be at the saturation temperaure of steam T_{Cj}, at the pressure in the steam chest. For the first effect, the mass of condensate $\mathcal{M}_{C1}$ in the lines between the steam chest for the first effect and the condensate flash tank for the second effect is concentrated in a perfect mixer. For all rate of heat transfer calculations, the steam in each effect is taken to be at T_{Cj}, except for the first effect, where it is taken to be equal to the saturation temperature T_{CO} of the supply steam. However, superheat if present in the steam entering the steam chest of a given effect is taken into account in the enthalpy balances.

10. The effect of noncondensables on the operation of the system of evaporators is taken to be insignificant because of the venting of the steam chest of each effect.

11. The mass of vapor (steam) in the steam chest in the evaporator and in the feed preheater as well as the vapor in the condensate-flash tank is taken to be negligible relative to the mass of condensate associated with each effect.

12. The mass of sea water feed in the preheater and preheater-feed lines between effects j and $j - 1$ is taken to be concentrated as the mass $\mathcal{M}_{Fj}$ of a perfect mixer as shown in Figures 2, 8, 9, and 22.* For all effects except the last one, wherein the holdup is associated with the acid treater, the mass of the holdups is taken to be independent of time. This assumption reflects the fact that the feed lines between effects were full at all times. The mass of metal in the feed lines associated with effect j is taken to be concentrated in the mass M_{Fj} at the temperature T_{Fj} of the perfect mixer. In the first effect, mass M_{F1} includes part of the mass of metal of the preheater. For the last effect, mass M_{F17} includes part of the mass of metal of the acid treater. This assumption is consistent with the fact that a change in temperature at a point in the piping has a magnitude and a time response similar to

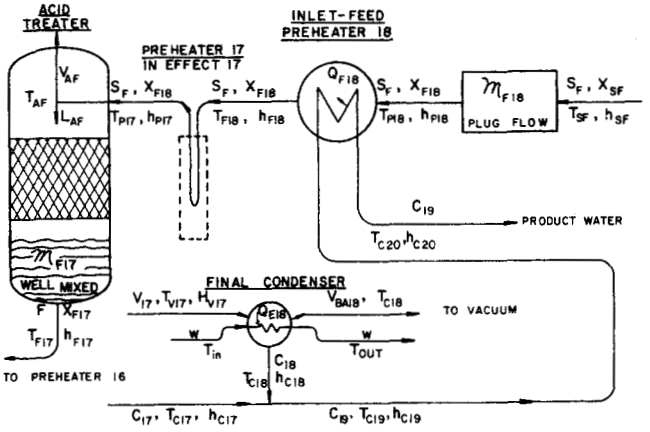

Fig. 9. Composite model of peripheral equipment in the evaporator system.

that predicted by the temperature T_{Fj}.

13. The dynamic behavior of the feed preheaters may be represented at any instant by the equations describing the steady state behavior of heat exchangers.

14. The mass of process liquid in the sump and in the lines associated with effect j is taken to be concentrated in the sump with a mass denoted by $\mathcal{M}_{Lj}$. This mass of liquid is taken to be perfectly mixed at the temperature T_{Lj} but not necessarily in thermal equilibrium with the vapor steam V_{Ej}.

15. For sump-to-sump flow, the process liquid stream L_{j-1} upon entering the sump of effect j is assumed to flash adiabatically at the pressure in the sump as indicated by the model of the adiabatic flash.

16. The instantaneous flow rate of the condensate from the flash tank of effect j to the flash tank of effect $j + 1$ is given by the corresponding fluid flow relationships for steady state flow. This assumption is based on the fact that the pipes were full of an incompressible fluid at all times and that the response time of the fluid flow portion of the system was negligible relative to the response times for other process variables.

17. The masses of the metal components associated with the preheater of the first effect are taken to be concentrated either in mass M_{C1} at temperature T_{C1} or in mass M_{F1} at T_{F1}. The concentrated masses are taken to be located in the perfect mixers of the model for the preheater as shown in Figure 8.

18. The dynamic values of the variables for the final condenser (see Figure 9) are related by the conventional steady state equations.

19. The holdup of energy in the metal masses associated with the final condenser and feed preheater 18 is assumed to be constant. This assumption is based on the fact that large upsets in the major process variables produced only small changes in the temperatures in the final condenser and in preheater 18.

20. The acid treater (see Figure 9) is represented in the process as an adiabatic flash process wherein the amount of sea water flashed is held constant by regulating the flow rates of the stripping steam entering and leaving the tower. For the evaluation of steady state conditions, the amount of sea water flashed is regulated to achieve a preassigned drop in temperature of the vapor leaving relative to the feed entering the flash process. For the evaluation of the transient behavior following an upset, the amount of sea water flashed is assumed to be constant at the value established during the steady state period preceding the upset. The holdup of liquid in the acid treater is taken to be regulated by means of a proportional controller during unsteady state operation.

* See footnote on page 1084.

21. Flow rates of the process liquid between evaporators are taken to be regulated by proportional controllers that detect changes in the mass holdup $\mathcal{M}_{Lj}$. Because of the noncylindrical shapes of the sumps, the mass $\mathcal{M}_{Lj}$ is not linear with the level measurement. Therefore the proportionality factor of each controller is made a function of $\mathcal{M}_{Lj}$ in the numerical treatment in order to correct for this nonlinearity.

22. To allow for the holdup of the feed in the piping between the feed pump (where the upsets in the feed composition occurred) and the evaporator module, a plug-flow section with holdup $\mathcal{M}_{F18}$ is assumed to exist, as indicated in Figure 9. This holdup is positioned before preheater 18 because most of the estimated holdup actually occurs there.

23. If any holes develop in the evaporator tubes of an effect, leakage of condensate and vapor occurs from the steam chest into the evaporator tubes. Provision for setting the condensate leakage rate C_{Lj} is provided in the model as shown in Figures 2 and 21.* Allowance for vapor leakage is made by adding any estimated leakage to the estimate for the vapor bleed V_B. Both of these leakage parameters were estimated from an analysis of steady state data.

FORMULATION AND SOLUTION OF THE EQUATIONS REQUIRED TO DESCRIBE THE MODEL FOR THE SYSTEM OF EVAPORATORS

Based on the assumptions stated, the equations required to describe each part of the model for the system were developed (3); these equations are also available elsewhere.* To demonstrate the procedures used, equations for two parts of the model are developed below.

Energy Balances on the Masses of Metal Walls Exposed To Steam (or Condensate) and the Surroundings

As indicated in Figures 2 and 19,* these balances include the metal walls which were in contact with steam on one side and the surroundings on the other side. The relatively small amount of metal which was in contact with condensate instead of steam was also included in this energy balance. In view of Assumptions 2 and 3, the energy balance over the time period from t_n to $t_n + \Delta t$ for any evaporator effect j $(1 \leqq j \leqq 17)$ is given by

$$\int_{t_n}^{t_n+\Delta t} [Q_{WSj} - Q_{ASj}]dt = M_{WSj}h_{WSj}|_{t_n+\Delta t} - M_{WSj}h_{WSj}|_{t_n} \quad (16)$$

When the implicit method (*5, 17*) is used to approximate the integral on the left-hand of Equation (16), the following result is obtained upon rearrangement:

$$\mu[Q_{WSj} - Q_{ASj}] + (1-\mu)[Q^\circ_{WSj} - Q^\circ_{ASj}] - \frac{M_{WSj}[h_{WSj} - h^\circ_{WSj}]}{\Delta t} = 0 \quad (17)$$

where the μ is the weight factor which may be arbitrarily selected as any number lying between 0 and 1. The superscript $^\circ$ is used to denote the values of the variables at the beginning of the time period under consideration, and the absence of a subscript is used to denote the values of the variables at the end of the time period under consideration. The rates of heat transfer to and from the metal wall are given by

$$Q_{WSj} = (UA)_{SW1}(T_{CO} - T_{WS1});$$
$$Q_{WSj} = (UA)_{WSj}(T_{Cj} - T_{WSj}), \quad (2 \leqq j \leqq 17); \quad (18)$$
$$Q_{ASj} = (UA)_{ASj}(T_{WSj} - T_A), \quad (1 \leqq j \leqq 17).$$

where $1/(UA)_{WSj}$ and $1/(UA)_{ASj}$ consist of the resistances offered to heat transfer in accordance with the heat transfer shown in Figure 19.*

Material and Energy Balances on the Contents in the Evaporator Tubes

These balances are based on Assumptions 1, 5, 6, 7 and 8. The model for this portion of the system is presented in Figures 2, 18,* and 21. In this case the holdup of mass and energy in the evaporator tubes is taken to be negligible, and thus the accumulation of energy [see, for example, the right-hand side of Equation (16)] is equal to zero for all choices of t_n and $t_n + \Delta t$. Consequently the integral of the input/time minus the output/time [see, for example, the left-hand side of Equation (16)] is equal to zero for all choices of t_n and $t_n + \Delta t$ in the time domain of interest. Thus the integrand is identically equal to zero for all t. For such cases, the energy or material balance is stated in its instantaneous form corresponding to the end of the time period under consideration. The material and energy balances as well as the boiling point elevation expressions for the process liquid in the evaporator tubes follow.

$$FX_{F1} - L_{E1}X_{E1} = 0$$
$$\alpha_{j-1}L_{j-1}X_{L,j-1} + L_{Rj}X_{Lj} - L_{Ej}X_{Ej} = 0, \quad (2 \leqq j \leqq 17)$$
$$F - L_{E1} - V_{E1} + C_{L1} = 0$$
$$\alpha_{j-1}L_{j-1} + L_{Rj} - L_{Ej} - V_{Ej} + C_{Lj} = 0, \quad (2 \leqq j \leqq 17) \quad (19)$$
$$Fh_{F1} + Q_{E1} - L_{E1}h_{E1} - V_{E1}H_{E1} + C_{L1}h_{CL1} = 0$$
$$\alpha_{j-1}L_{j-1}h_{L,j-1} + L_{Rj}h_{Lj} + Q_{Ej} - L_{Ej}h_{Ej} - V_{Ej}h_{Ej} + C_{Lj}h_{CLj} = 0, \quad (2 \leqq j \leqq 17)$$

where

$$Q_{E1} = (hA)_{E1}(T_{CO} - T_{E1});$$
$$Q_{Ej} = (hA)_{Ej}(T_{Cj} - T_{Ej}), \quad (2 \leqq j \leqq 17).$$

The temperature T_{Ej} of the liquid in the evaporator tubes is computed by using Dühring lines, which may be represented as follows:

$$m\,T_{C,j+1} + b - T_{Ej} = 0, \quad (1 \leqq j \leqq 17) \quad (20)$$

where the slope m depends upon both X_{Ej} and $T_{C,j+1}$, and b depends upon X_{Ej} alone; that is, $m = m(X_{Ej}, T_{C,j+1})$ and $b = b(X_{Ej})$.

ANALYSIS OF THE RESULTS OF FIELD TESTS

The predicted behavior of the plant at a given set of operating conditions and physical parameters was obtained by solving the equations of the model for the values of the independent variables at the end of each time step. The complete mathematical model consisted of 380 equations of the same general form as those shown for Equations (16) through (20) in 380 unknowns. These equations were solved simultaneously for the variables at the end of each time step by use of the Newton-Raphson

* See footnote on page 1084.

* See footnote on page 1084.

method (5, 17). A generalized scaling procedure was employed.* Also, in order that any $\Delta t > 0$ might be used at any point in the sequence of calculations without having the inherited error become unbounded, a $\mu = 0.6$ was used. The selection of this value of μ was based on the results of a preliminary study of the dynamics of a single-effect evaporator. In this study it was shown that the inherited error was bounded, provided $0.5 \leqq \mu \leqq 1$.

The program for the unsteady state model could be used to obtain the steady state solution for the given set of operating conditions by setting $\mu = 1$ and by setting $\Delta t = 10^{30}$ hr. This choice of values for μ and Δt had the effect of the elimination of the input and output terms at the beginning of the time step as well as the elimination of the accumulation terms and thereby gave the steady state equations corresponding to the final steady state. In the application of the Newton-Raphson method, approximations were used for certain of the partial derivatives. In particular, the partial derivatives of the liquid enthalpies with respect to the salt content were taken equal to zero.

On the average, about four iterations of the Newton-Raphson method were required per time step. About 15 iterations were required to solve the initial steady state problems. More trials were required to solve the steady state problem than were required for any time step of the unsteady state problem because the initial guesses for the steady state problem were poorer than those for the unsteady state problem. The initial guesses for the steady state problem were obtained by use of a relatively simple scheme which was similar to those commonly used; see, for example, Perry (22). The initial guesses for the values of the variables at the end of each time step consisted of taking them equal to the values of the variables which were found at the end of the previous time step.

Determination of Equipment Parameters

Physical dimensions of the holdup volumes, the surface areas, the masses of metal, and the types of material of the heat sinks were obtained from the construction blueprints of the plant. Since effective values were needed in the model, some personal judgment was used in assigning part or all of a mass (or volume) to its counterpart in the process model.

Heat transfer areas for the tubes of the preheaters and evaporators were obtained from the status records of the plant equipment. Coefficients of heat transfer for the various exchangers were determined from the results of recent steady state test runs performed and reported by the plant personnel. Since the coefficients of heat transfer for LTV evaporators vary with operating temperature (26, 27), the values used in the numerical evaluation of the mathematical model were adjusted for the effect of temperature by use of the relationship reported by Standiford (27). In particular, the derivative of the heat transfer coefficient h_{Ej} with respect to T_{Ej} was taken equal to the slope of the line given by Standiford (27).

Other film coefficients* employed were computed by use of relationships given by Perry (22). Physical properties of the metal walls, tubing, piping, and the insulation were taken from Perry (22), as well as the thermodynamic and physical properties of steam and water. Enthalpies, specific heats, and boiling point elevations of the brine process liquid were taken from references 2 and 25. The data and parameters used in the model are presented in Appendix C.*

Test Run 1 consisted of a sequence of upsets in the salt concentration of sea water feed; see Table 1. These

Table 1. Operating Conditions of the Evaporator System for Test Run 1

Parameter	Initial value
Sea water feed rate, M lb./hr.	480
Concentration of brine in feed, C.F.	0.935
Temperature of feed, °F.	82
Temperature of steam to effect No. 1, °F.	300
Dew point in first steam chest, °F.	270
Steam rate to first steam chest, M lb./hr.	26
Cooling water supply rate, M lb./hr.	986
Temperature of cooling water, °F.	82
Temperature of atmospheric air, °F.	80
Control method for steam = pressure	

Upset schedule					
Time, min.	Upset variable	New value	Type of change	Time constant, min.	Step size, min.
0	C.F. of feed	0.692	Linear	1.0	0.5
7	C.F. of feed	0.632	Linear	0.5	0.5
10	C.F. of feed	0.560	Linear	0.5	0.5
25	C.F. of feed	0.756	Linear	0.0	1.0
30					2.0
50					5.0
80					10.0

upsets were achieved by diluting the incoming sea water with product water from the plant. Samples of the process liquid were taken at the outlets of the feed pump, the acid treater, and the evaporator sumps. Flow rates, temperatures, and sump levels were monitored and recorded by instruments in the control system.

Salt content of each sample was determined by measuring its refractive index. The refractive index was calibrated against the salt content as determined by titration of the calibration samples with silver nitrate. The salt content of the samples was expressed in terms of the concentration factor (C.F.), which represented the ratio of the chlorinity of the sample to the chlorinity of normal sea water (10). Chlorinity is the total amount of chlorine (grams) contained in 1 kg. of sea water in which all of the bromide and iodide have been replaced by chloride.

Two sets of variables were used for the comparison of the experimental and calculated results of this field test run, namely, the vapor temperatures and the salt concentrations of the brine process liquid. The temperatures of the vapors leaving effects 1 through 12 were monitored during the transient operation by means of thermocouples located in the vapor lines leaving each effect. Salt concentrations were determined for the samples which were withdrawn from the discharge side of pumps used to transfer (or recycle) the brine process liquid.

Prior to making Run 1, the plant was brought to a steady state with the process variables at typical operating levels, and then the salt concentration of the feed was upset as shown in Table 1. Operation specifications and parameters for the system of evaporators are shown in Appendix C.* Temperatures of the exit vapors and the concentrations of the brine process liquid leaving the sumps at the initial steady state are presented in Table 2. The average deviation between the measured and the calculated temperatures for the first 12 effects was 1.9°F. If the temperatures indicated by the thermocouples were dew point temperatures rather than the actual temperatures of the superheated vapors, then the measured temperaures should be compared to the condensate temperatures of the steam

* See footnote on page 1084.

* See footnote on page 1084.

chests of the next effect. When such a comparison was made, an average deviation of 0.9°F. was obtained for the first 11 effects, and a deviation of 4.4°F. was obtained for the twelfth effect. The higher deviation for the twelfth effect was attributed to the low value of the heat transfer coefficient use in the calculation; see Table 5.* Thus the agreement between the measured and calculated temperatures was relatively good, without making any adjustment of the heat transfer coefficients or vent rates.

The experimental salt concentrations of the brine process liquid which flowed from the sumps of the evaporators were in good agreement with the values calculated by use of the model; see Table 2. The good agreement between the calculated and observed concentrations at steady state operation implies that the agreement between the actual and the calculated flow rates of the brine process liquid was also good.

Throughout the sequence of upsets in the salt concentrations of the feed, the temperatures and flow rates of the process streams remained relatively constant. The concentration of salt in each of the process liquid streams leaving each of the sumps varied with time as predicted by the model; see Figure 10. Samples of the various process liquid streams were taken at times at which it had been anticipated that the break-points of the time-concentration curves would be included. Levels of process liquid in the sumps were measured with differential-pressure transmitters, which were read by use of the display meters located in the control room. The flow of purge water through the pressure taps into the sumps caused significant errors in the determination of some of the liquid levels. Because of this difficulty, estimates of the actual levels were made by use of the break-points in the time-concentration curves. These estimated levels were utilized in the calculational procedure. In Table 7* both the measured levels recorded during the test and the estimated levels are listed.

The good agreement between the calculated and measured slopes of the time-concentration curves following the break-points (see Figure 10) demonstrates that the holdup of the process liquid is adequately described by the use of perfect mixers in the process model.

In a second sequence of upsets of the feed rate (called Test Run 2), good agreement between the observed and predicted behavior of the system of evaporators was obtained, as described elsewhere.*

No attempt was made to use the results of the test runs to obtain values of the parameters except for the level controllers on the evaporator sumps. Also, an estimate of the condensate leakage was made for Run 1 in order to account for inconsistencies in the brine concentrations which were observed at the initial steady state prior to the upset.

Thus the initial steady state values and the unsteady state values of the variables which were calculated by use of the model represent a fair evaluation of how well the steady state and dynamic response of a system of evaporators could be predicted by use of the proposed model.

Table 2. Steady State Vapor Temperatures and Brine Concentrations for Test Run 1

Effect No.	Temp. of exit vapors, °F. Measured at plant	Temp. of exit vapors, °F. Calculated from model	Conc. of brine from sump (C.F.) Plant sample	Conc. of brine from sump (C.F.) Calculated from model
1	262	262.8	0.97	0.98
2	262	255.3	1.02	1.03
3	246	246.9	1.08	1.08
4	239	240.0	1.13	1.13
5	231	231.6	1.18	1.18
6	223	224.5	1.24	1.25
7	214	216.7	1.30	1.32
8	206	209.1	1.38	1.39
9	197	199.1	1.46	1.47
10	186	188.9	——	1.56
11	176	178.3	1.66	1.67
12	167	165.2	1.78	1.78
13		155.5	1.89	1.90
14		144.1	2.05	2.05
15		133.0	2.22	2.21
16		122.0	2.39	2.39
17		110.4	2.58	2.54

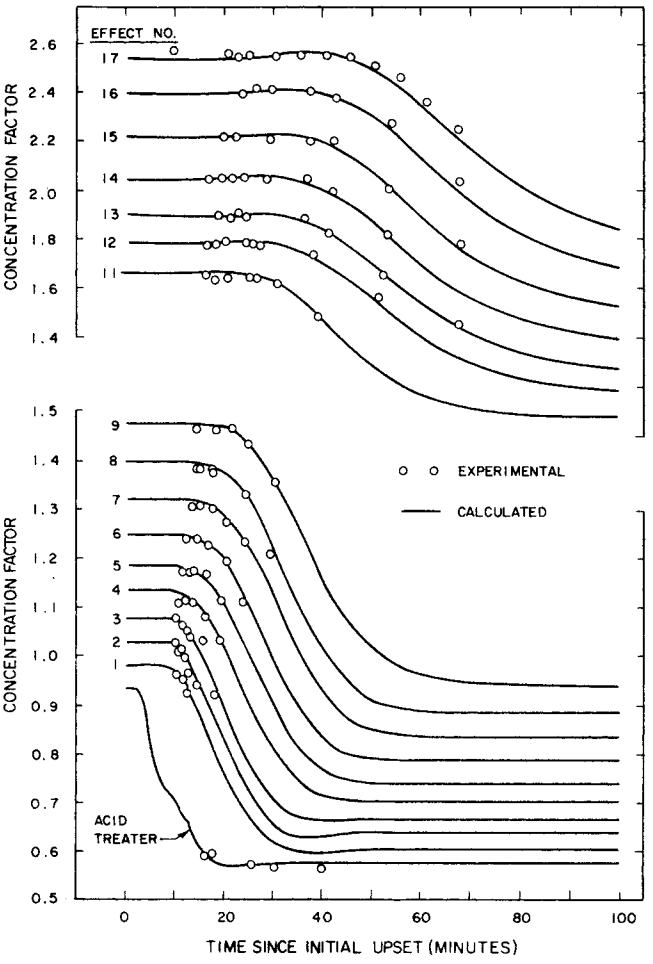

Fig. 10. Concentrations of brines leaving evaporators sampled during Test Run 1.

ACKNOWLEDGMENT

The support provided by the National Science Foundation and the Office of Saline Water, U.S. Department of Interior, is gratefully acknowledged. The assistance given by Charles Grua with the Office of Saline Water and J. P. Lennox, Keith S. Campbell, and Don L. Williams, all of Stearns-Roger Corporation, is appreciated.

NOTATION

a = constant as defined below Equation (7)
A = area perpendicular to the direction of heat transfer, sq. ft.

* See footnote on page 1084.

C_j = flow rate at which condensate leaves evaporator effect j, lb./hr.
C_n = constant as defined below Equation (7)
C_V, C_p = heat capacities at constant volume and constant pressure, respectively, B.t.u./(lb.)(°F.)
D_n = constant as defined below Equation (7)
h = enthalpy of a liquid phase B.t.u./lb. Also, the coefficient of heat transfer is denoted by this symbol and has the units of B.t.u./(hr.)(sq. ft.)(°F.)
H = enthalpy of the vapor phase, B.t.u./lb.
H_1, H_2 = constants as defined below Equation (7)
k = thermal conductivity, B.t.u./(hr.)(ft.)(°F.)
l = thickness of metal wall, ft.
L = flow rate of process liquid, lb./hr.; also used to denote the length in feet along the axis of a cylinder
m = slope of Dühring line; see Equation (20); also used to denote the mean value of a variable
$\mathcal{M}$ = mass of liquid holdup, lb.
M = mass of metal holdup, lb.
P_j = pressure in the vapor space of evaporator effect j, lb./sq. ft.
Q = rate of heat transfer, B.t.u./hr.
r = radius of cylindrical shell
S_F = sea water feed, lb./hr.
T = temperature, °F.
U = overall coefficient of heat transfer, B.t.u./(hr.)(sq. ft.)(°F.)
V = flow rate of vapor. lb./hr.
w = flow rate of coolant to the final condenser, lb./hr.
X = mass fraction of the solute
Y_n = function as defined below Equation (7)

Greek Letters

α_j = fraction of the liquid L_j entering the tubes of evaporator effect j (see Figure 2); also used to represent the ratio $(k/\rho C_v)$ in Equation (5)
β_n = n^{th} positive root of the equation presented below Equation (7)
ρ = density, lb./cu. ft.
π = 3.1416 radians
μ = weighting factor for the implicit method

Mathematical Symbols

$[f(t)]^\circ$ = value of the function $f(t)$ at the beginning of the time period under consideration

$\text{erfc}\, z = \frac{2}{\sqrt{\pi}} \int_z^\infty e^{-\gamma^2} d\gamma$, the complementary error function

$\text{ierfc}\, z = \int_z^\infty \text{erfc}\, \xi\, d\xi = \frac{e^{-z^2}}{\sqrt{\pi}} - z\, \text{erfc}\, z$, the integral of the complementary error function

Subscripts

av = arithmetic average
A = surroundings or ambient conditions
AF = adiabatic flash of the sea water feed
AF_j = adiabatic flash of the process liquid $(2 \leqq j \leqq 17)$
B = bleed
BA = bleed to the surroundings
C = saturation conditions for steam
E = evaporate; also refers to the conditions in the tubes of an evaporator
F = feed
IC = intermediate condition of the condensate leaving the first effect (see Figure 8)
j = effect number (j = 1, 2, 3, . . . , 17), and subscripts j = 18, 19, and 20 refer to streams treated by peripheral equipment
L = process liquid at the conditions in the sump
P = condition of the feed leaving a feed preheater; see Figures 2 and 8
S = steam
V = vapor
WS = variables associated with the transfer of heat from steam to a metal wall; also used to denote the mean temperature of the wall. The symbol AS refers to the transfer of heat from this wall to the surroundings

LITERATURE CITED

1. Bonilla, C. F., *Trans. AIChE.*, **41**, 529 (1945).
2. Bromley, L. A., V. A. Desaussure, and J. C. Clipp, *J. Chem. Eng. Data*, **12**, 203 (1967).
3. Burdett, J. W., Ph.D. dissertation, Texas A&M Univ., College Station (1970).
4. Campbell, K. S., Stearns-Roger Corp., personal communication (1968-70).
5. Carnahan, B., H. S. Luther, and J. O. Wilkes, "Applied Numerical Methods," Wiley, New York (1969).
6. Carslaw, H. W., and J. C. Jaeger, "Conduction of Heat in Solids," 2nd edit., Oxford Univ. Press, New York (1959).
7. Carter, A. L., and R. R. Kraybill, *Chem. Eng. Progr.*, **62**, 99 (1966).
8. Churchill, R. V., "Operational Mathematics," 2nd edit., McGraw-Hill, New York (1958).
9. Detman, R. F., *Chem. Eng. Progr.*, **63**, 81 (1967).
10. Dykstra, D. I., *ibid.*, **61**, 80 (1965).
11. *Expanded Partial Enthalpy Tables for Water in Sea Water and NaCl in Aqueous Solution*, Stearns-Roger Corp. Rept. for U.S. Dept. Interior, Office Saline Water (1966).
12. *Fifth Annual Report, Sea Water Desalting Plant and Distillation Development Facility*, Stearns-Roger Corp. Rept. for U.S. Dept. Interior, Office Saline Water (1966).
13. Franks, R. G. E., and W. E. Schiesser, *Chem. Eng. Progr.*, **63**, 68 (1967).
14. *Freeport Plant ME-LTV Operations*, Saline Water Conversion Rept., p. 253, Supt. Documents, U.S. Government Printing Office, Washington, D. C. (1966).
15. Galstaun L. S., and E. L. Currier, *Chem. Eng. Progr.*, **63**, 65 (1967).
16. *Heat Transfer in Vertical-Tube Evaporation*, Saline Water Conversion Rept., p. 190, Supt. Documents, U.S. Government Printing Office, Washington, D. C. (1966).
17. Holland, C. D., "Unsteady State Processes with Applications in Multicomponnet Distillation," Prentice-Hall, Englewood Cliffs, N. J. (1966).
18. Huang, C. J., H. M. Lee, and A. E. Dukler, *Desalination*, **6**, 6 (1968).
19. Itahara, S., and L. I. Stiel, *Ind. Eng. Chem. Process Design Develop.*, **7**, 6 (1968).
20. McCabe, W. L., *Trans. AIChE*, **31**, 129 (1934).
21. *Optimum Design of Long-Tube-Vertical Plants*, Saline Water Conversion Rept., p. 188, Supt. Documents, U.S. Government Printing Office, Washington, D.C. (1966).
22. Perry, R. H., C. H. Chilton, and S. C. Kirkpatrick, ed., "Chemical Engineers Handbook," 4th edit., McGraw-Hill, New York (1963).
23. Phillips, J. C., *Chem. Eng.*, **70**, 97 (Apr. 1963).
24. Rosenbrock, H. H., *Chem. Eng. Progr.*, **58**, 43 (1962).
25. *Saline Water Conversion Engineering Data Book*, Supt. Documents, U.S. Government Printing Office, Washington, D.C. (1965).
26. Standiford, F. C., and H. F. Bjofk, *Chem. Eng. Progr.*, **63**, 70 (1967).
27. Standiford, F. C., *Chem. Eng.*, **70**, (25), 157 (1963).

Manuscript received March 10, 1970; revision received July 24, 1970; paper accepted July 29, 1970.